Scripta Materialia 113 (2016) 71–74

Contents lists available at ScienceDirect

Scripta Materialia

journal homepage: www.elsevier.com/locate/smm

Buckling failure in air-plasma sprayed thermal barrier coatings induced by molten silicate attack

Xiao Shan [a], Zhonghua Zou [a], Lijian Gu [a], Lixia Yang [a], Fangwei Guo [a], Xiaofeng Zhao [a,*], Ping Xiao [b]

[a] Shanghai Key Laboratory of Advanced High-Temperature Materials and Precision Forming, Shanghai Jiao Tong University, Shanghai 200240, China
[b] School of Materials, University of Manchester, Grosvenor Street, Manchester M1 7HS, UK

ARTICLE INFO

Article history:
Received 18 June 2015
Received in revised form 14 September 2015
Accepted 19 September 2015
Available online 24 October 2015

Keywords:
Thermal barrier coatings
Air-plasma spray
Buckling
Liquid infiltration
Calcium–magnesium-alumino-silicate

ABSTRACT

The buckling phenomenon in air-plasma sprayed yttria-stabilized zirconia (YSZ) thermal barrier coatings (TBCs) induced by calcium–magnesium-alumino-silicate (CMAS) attack was investigated. The liquid CMAS infiltration due to capillary force weakened the interface and introduced a significant volume expansion (32%) in the top coat, leading to a large scale buckling of the TBC at high temperature. The dissolution and tetragonal-mononiclic phase transformation of YSZ induced by CMAS only has a negligible contribution.

Thermal barrier coatings (TBCs) have been widely used to provide thermal insulation for metallic components operating in hot section of gas turbines used for aircraft propulsion and power generation [1–3]. It helps increase the entry temperature and thereby the efficiency of the engines. However, calcium–magnesium-alumino-silicate (CMAS) attack is becoming a more critical issue with ever-increasing demand for higher operating temperature in future high-efficiency gas-turbine engines [3,4]. CMAS usually comes from siliceous debris such as sand, volcanic dust, and fuel residue [5]. Large siliceous debris can cause impact damage to TBCs, while small debris can cause erosive wear or local spallation [6–10]. When the surface temperature of TBCs exceeds the CMAS melting point, the siliceous particles penetrates into TBCs due to remarkable wetting ability [6,11,12]. Yttria-stabilized zirconia (YSZ) is then partially dissolved by CMAS, resulting in microstructure degradation and phase transformation [13]. The porosity is reduced, leading to an increase of the thermal conductivity and stiffness [14,15]. CMAS was also observed to penetrate down to the substrate and attack the thermally grown oxide (TGO), promoting detachment of TBCs [12]. CMAS attacks TBCs primarily via cold shock degradation mechanism [16]. Upon cooling, CMAS solidifies, and the in-plane modulus of the CMAS-penetrated layer increases by a factor of 5–10 [16]. Such high modulus and low toughness of TBC increase its susceptibility to cracking during engine shutdown [16]. Cumulative cracks promoted by engine cycles lead to final spallation of TBCs [17].

Generally, failure of plasma sprayed TBCs through buckling has been rarely observed [18,19]. However, as will be shown in this work, the air-plasma sprayed (APS) TBC can be buckled severely after CMAS infiltration. Therefore, the objective of this study is to investigate this phenomenon and understand the buckling mechanism of APS TBCs under CMAS attack.

The specimens used are standard APS TBCs, which consist of a 8YSZ top coat (16% porosity), an APS NiCoCrAlY bond coat (roughness Ra ~6 μm), and a Hastelloy-X substrate. The thickness of the top coat was ~210 μm. The chemical composition of CMAS was 33CaO–9MgO–13$AlO_{1.5}$–45SiO_2 mol% (glass transition and melting temperatures are respectively 764 °C and 1233 °C [20]), which was prepared by mixing fine powders of individual oxides and attrition milling them in isopropanol to form a thick paste. Afterwards, the CMAS paste was applied on the top coat. To avoid spallation of whole coating, only a small circular region (~2 mm in diameter) in the middle was covered by CMAS. After drying, the amount of CMAS was controlled to 18 mg/cm^2. This value was estimated based on the porosity of the coating and expected to be sufficient to fill all the pores. Then the specimens were heat-treated in a chamber furnace to 1250 °C for 4 h, and cooled to room temperature, with a heating/cooling rate of 5 °C/min. This temperature was used because it is higher than the melting temperature of CMAS (1233 °C [20]) and close to the operating temperature (~1250 °C) of TBCs [21]. For comparison, an APS TBC (16% porosity) cut from the same specimen was also heat-treated at the same condition but without CMAS.

To get a more accurate quantification of the CMAS infiltration, a free-standing APS TBC (7.1 × 5.0 mm^2) with 14% porosity was prepared. The

* Corresponding author.
E-mail address: xiaofengzhao@sjtu.edu.cn (X. Zhao).

http://dx.doi.org/10.1016/j.scriptamat.2015.09.029
1359-6462/

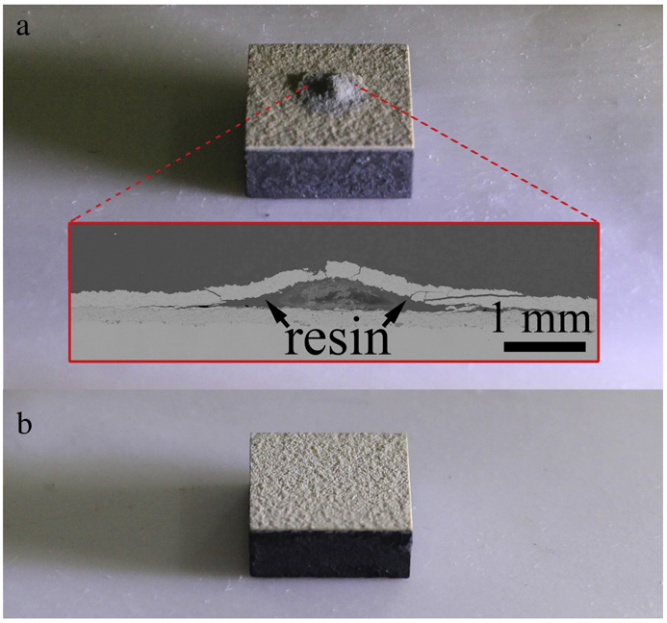

Fig. 1. Optical images of APS TBC after heat treatment at 1250 °C for 4 h (a) with and (b) without CMAS. The inset in (a) is the cross-sectional image of the coating after CMAS attack.

substrate was removed using aqua regia. Both the top and bottom surface were grinded to achieve a uniform thickness (254 μm). Then the CMAS paste was applied on the whole surface. The amount of CMAS was controlled to 25 mg/cm^2 after drying, which is far beyond the amount needed to fill all the porosity in this coating. Note that more CMAS was applied and the heat treatment time (9 h) was longer because the freestanding coating is thicker than the coating with substrate and greater expansion is needed for more precise calculation. The freestanding coating was heat-treated to 1250 °C (5 °C/min) for 9 h, and then cooled to room temperature. For comparison, a freestanding APS TBC (7.0 mm × 4.8 mm × 254 μm) with 14% porosity was also heat-treated at the same condition but without CMAS.

The microstructure of the specimens was observed using a scanning electron microscopy (SEM). All specimens were prepared using the standard metallographic procedure. The chemical composition was determined using energy dispersive spectroscopy (EDS). A Raman microscope (HR evolution, Horiba) with an excitation of 532 nm (Ar laser) and X-ray diffraction (XRD) was used to measure the monoclinic phase distribution of the coating.

Fig. 1a presented the optical image of a supported APS TBC after CMAS attack at 1250 °C for 4 h. In this case, only a small circular region in the middle was covered by CMAS. The cross-section of the coating was shown as inset. The buckling of APS TBC was evident. The delamination mainly occurred around the CMAS covered region, from the YSZ/TGO interface. The length of the buckled top coat increased by 11%. In contrast, no buckling was observed in the reference APS TBC (Fig. 1b).

Fig. 2a shows an optical image of the freestanding APS TBC after CMAS attack at 1250 °C for 9 h. In this case, the whole surface was covered by CMAS. Assuming a spherical shell, the volume was estimated as 11.9 mm^3, 32% larger than its original volume (9.0 mm^3). The high-magnification image of the coating (Fig. 2b) shows that there is no residual CMAS on its surface, indicating that all CMAS has infiltrated into the coating. It implies that the amount of infiltrated CMAS is not limited

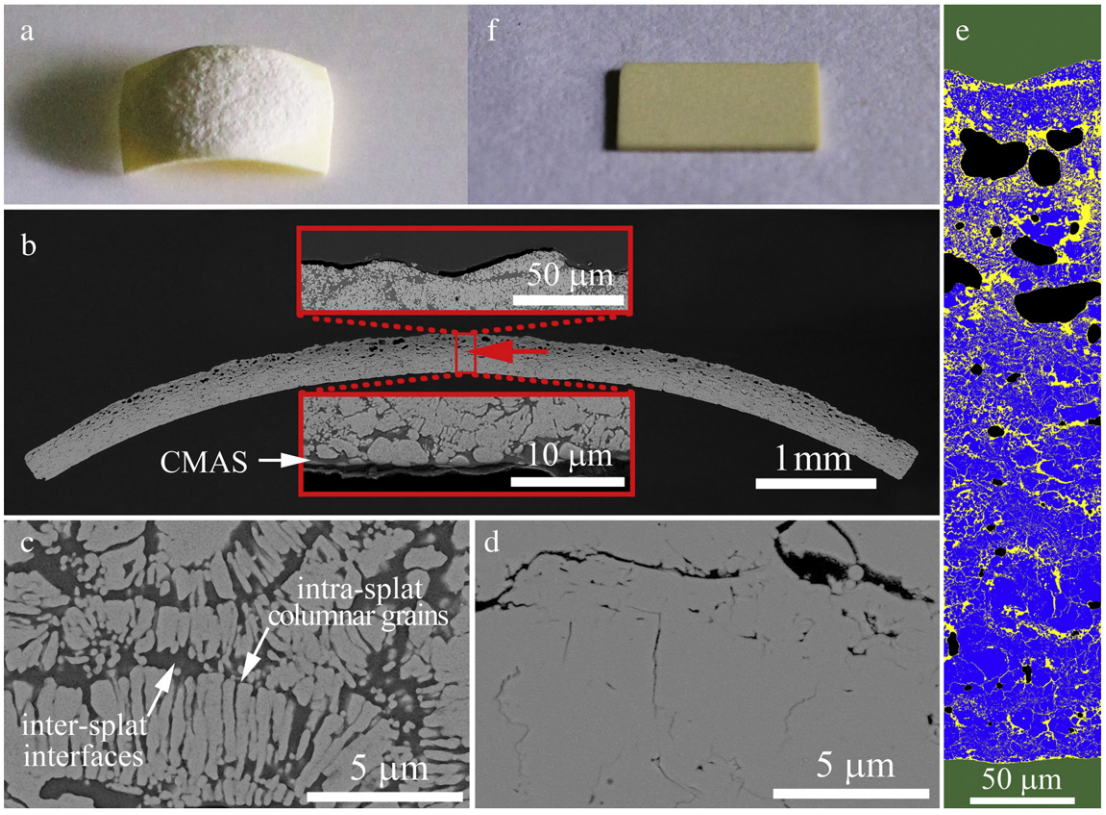

Fig. 2. (a and f) Overview of the freestanding APS TBC heat-treated at 1250 °C for 9 h with (a) and without (f) CMAS. (b) Cross-sectional images of the coating after CMAS attack. The enlarged region of the top surface and the bottom were shown as insets. (c) High-magnification image of the region marked by the red arrow in (b), showing the inter- or intra-splat boundaries were separated by CMAS. (d) The original microstructure of the APS TBC without CMAS attack. (e) Image showing the distribution of CMAS (yellow), YSZ (blue) and pores (black) in the region marked by the red rectangle in (b).